Active Region Properties and Irradiance Variations

Tünde Baranyi*

Heliophysical Observatory of the Hungarian Academy of Sciences, P.O.Box 30, Debrecen, H-4010, Hungary

Judit M. Pap

The Catholic University of America, c/o NASA/Goddard Space Flight Center, Code 612.1, Greenbelt, MD 20771, USA

Abstract

Total solar irradiance (TSI) has been measured for more than three decades. These observations demonstrate that total irradiance changes on time scales ranging from minutes to years and decades. Considerable efforts have been made to understand the physical origin of irradiance variations and to model the observed changes using measures of sunspots and faculae. In this paper, we study the short-term variations in TSI during the declining portion and minimum of solar cycle 22 and the rising portion of cycle 23 (1993 – 1998). This time interval of low solar activity allows us to study the effect of individual sunspot groups on TSI in detail. In this paper, we indicate that the effect of sunspot groups on total irradiance may depend on their type in the Zürich classification system and/or their evolution, and on their magnetic configuration. Some uncertainties in the data and other effects are also discussed.

Keywords: Solar activity; Solar irradiance; Solar variability

1. Introduction

The solar radiation is the main driver of the radiative, photochemical and dynamical processes in the Earth's atmosphere. Therefore, understanding

*Corresponding author

Email addresses: baranyi@tigris.unideb.hu (Tünde Baranyi), judit.m.pap@nasa.gov (Judit M. Pap)

and predicting the variations in total solar irradiance (TSI) is one of the key issues in solar-terrestrial physics since they may have a direct impact on climate change. To fully understand the response of the Earth's atmosphere and climate system to irradiance changes, accurate and long-term total irradiance measurements are required (e.g. Krivova et al., 2011; Schmidt et al. 2011). Total solar irradiance has been observed from space since late 1978, starting with measurements on-board the Nimbus-7 satellite. Investigations of these observations have demonstrated that TSI changes on time scales ranging from minutes to the entire 11-year solar cycle. The recent review by Domingo et al. (2009) discusses the irradiance measurements, reconstructions, and related mechanisms.

On time scales of minutes to hours, the effect of granulation, meso-, and supergranulation has been recognized in solar irradiance, whereas the rapid irradiance fluctuations in the 5-minute range are due to the p-mode oscillations (e.g. Fröhlich *et al.*, 1997). On longer time scales, the solar surface magnetic features (spots, faculae, and network) play the dominant role in irradiance variations. Although the physical origin of the observed irradiance variations is basically understood, and the recent irradiance reconstructions describe the measured irradiance fairly well, there do remain differences between models and observations. The origin of these residuals may be related to various effects, such as observational uncertainties, unrevealed solar effects, and/or insufficient modeling efforts. While it is clear that sunspots cause negative excursions and faculae cause temporary increases in total solar irradiance on active region time scales (days to months), the role of the evolution of active regions in irradiance variations is not yet well-understood.

In this paper, we address a specific but important question: Does the evolution and morphology of individual sunspot groups affect TSI? Our investigation is carried out for the time interval of 1993 to 1998, which represents the declining portion and minimum of solar cycle 22 and the rising portion of solar cycle 23. This time interval was selected because the relatively low level of solar activity would facilitate the identification of individual sunspot groups and their effect on total irradiance.

2. Data description

In our analysis, we have used the the UARS/ACRIM II TSI (Willson and Mordvinov, 2003), shown in Figure 1e. Because of the lack of spatially resolved photospheric facular data, we have used the Mg core-to-wing ratio

(hereafter Mg c/w) as a proxy for faculae (Figure 1b). Mg c/w is the ratio of the chromospheric core to the photospheric wings of the compound Mg II absorption line measured in the vicinity of the 280 nm UV irradiance. This index is considered a reasonably good indicator for the changing emission of faculae and other bright solar features (Heath and Schlesinger, 1986; Floyd et al., 2005).

Sunspot data used in this study are coming from the Debrecen Photoheliographic Data (DPD) catalog, which is compiled as a continuation of the Greenwich Photoheliographic Results (GPR) (Győri et al. 2005, 2011). To analyze the full-disk white-light or continuum images, the Sunspot Automatic Measurement (SAM) program has been developed (Győri, 1998) which is a set of cooperative computer programs to compile a sunspot catalog. The basic data in a sunspot catalog are the heliographic positions and the areas of the sunspots. Full-disk white-light images and magnetic observations are also appended to the DPD.

To describe the effect of sunspots on solar irradiance, the Photometric Sunspot Index (PSI) was developed at the beginning of the irradiance observations (e.g. Hudson et al., 1982). PSI depends on the area, the location (in heliocentric coordinates), and the photometric contrast of sunspots (the brightness of the spot relative to the surrounding photosphere), and it is summed over all spots on the visible solar disk. It describes the radiation deficit caused by the spots. We note that in the original definition of PSI, the contrast of sunspots was a constant value. Later, various studies showed that the contrast of sunspots varies as a function of their area (e.g. Steinegger et al, 1990). In this study we have used contrast-area relationship between average sunspot contrast C_a and the total sunspot area A_s as defined by Wesolowski et al. (2008), where $C_a = 0.049 * logA_s + 0.017$. To calculate the contrast and PSI, the A_s sunspot area and position data of sunspots are taken from the DPD catalogue. PSI is shown in Figure 1a.

To gain more insight into the effect of individual sunspot groups on TSI, we identified those days when only one sunspot group was present on the visible solar disk. However, this strict criterion would allow only a small statistical sample size, therefore we used the ratio of the projected area of the particular sunspot group to the daily sum of the projected area of all the visible groups as selection criterion. If this ratio is larger than 0.7, we assume that the actual irradiance is dominated by that largest group on the solar disk on the given day. Further criteria were that only those groups were selected which had a Central Meridian Distance (CMD, also called as

Longitude from the Central Meridian) smaller than 60 degrees in absolute value, and at least one sunspot had penumbra. With these constraints the statistical sample size is 662 dominant groups on 662 days. We emphasize that PSI is always calculated by using all the visible sunspots including even the smallest ones, but the day has a label referring to the dominant sunspot group.

To describe their morphology, the selected sunspot groups have been divided into various classes following the Zürich sunspot group classification (in the bracket the number of the selected sunspot groups in that class is indicated):

C (225) - A bipolar sunspot group. One sunspot must have penumbra.

D (185) - A bipolar sunspot group with penumbra on both ends of the group. Longitudinal extent does not exceed 10 deg.

E (139) - A bipolar sunspot group with penumbra on both ends. Longitudinal extent exceeds 10 degrees but not 15 degrees.

F (30) - An elongated bipolar sunspot group with penumbra on both ends. Longitudinal extent exceeds 15 degrees.

H (83) - A unipolar sunspot group with penumbra.

The information on the type of daily sunspot data in the Zürich classes has been taken from the USAF_MWL (USAF and Mount Wilson) sunspot region dataset published in the Solar Geophysical Data (SGD) catalogue by NOAA/NGDC. Sunspot data in the SGD catalogue come from several stations, and the sunspot classification sometimes differs from one station to another. This might be due to observational errors or due to the time difference. Because of the ambiguity, we have used the most frequently indicated class for a selected sunspot group for a given day as a "daily mean of Zürich class". In the most ambiguous cases, the classes of groups published in SGD were compared with the photospheric images and magnetograms appended to DPD, and the daily Zürich class of the group was corrected when needed.

To show the fraction of the contribution of the dominant group to PSI, we computed the value of the partial PSI calculated from the dominant sunspot group and divided by the PSI calculated from all the spots visible on the solar disk. The statistical distribution of these ratios is listed in Table 1. As can be seen, the dominant sunspot group always determines the largest fraction of PSI in each selected case and it is reasonable to assume that it has the dominant effect on TSI.

Table 1: The ratio of the partial PSI of the dominant sunspot group to the total PSI

r	Number of cases
$0.99 <= r$	298
$0.9 <= r < 0.99$	189
$0.8 <= r < 0.9$	129
$0.7 <= r < 0.8$	43
$0.67 <= r < 0.7$	3

3. Effect of sunspots on total irradiance

3.1. Method of analysis

Irradiance models based on linear regression analysis assume that variation in total irradiance can be described by a linear combination of darkening effect of sunspots and the excess flux of bright faculae. We note that this method of analysis cannot take into account the dynamics and non-linearity existing between irradiance variations and solar indices (Vigouroux et al., 1997; de Toma et al. 2001; Pap et al., 2002; Preminger and Walton, 2007). However, now our goal is not to create an excellent model but to have a simple tool to study the effects of various types of sunspot groups on TSI easily. In our analysis, we have used multiple linear regression analysis relating TSI to PSI and Mg c/w. We used the method of Fröhlich (2002) to determine the lower envelope of the Mg c/w ratio, and to separate the long-term (Mg_l) and short-term (Mg_s) variations of the Mg c/w ratio shown in Figure 1c and 1d. We calculated the lower envelope with an 81-day moving average (3 solar rotations) as the probable minimum of the size of the long-term window. In this three-component model TSI is modeled with the (Mg_l), (Mg_s) and PSI as $TSI = a + b * PSI + c * Mg_l + d * Mg_s$). The coefficient of determination R^2 of our model is 0.8, and Figure 1f shows the residuals between TSI and its model. As can bee seen, the proxies can remove only a fraction of the short-term variations.

Various causes can be identified of the residual variations in Figure 1f, such as (1) the uncertainty in the measurements, including irradiance, the Mg observations and the sunspot area and contrast measurements, (2) use of improper proxy data in the model, and (3) the modeling effort itself. We note that one of the largest obstacles of irradiance modeling is the lack of measurements of photospheric faculae both inside and outside of active regions. Thus, one has to rely on chromospheric indices, like the Mg c/w

ratio, to account for the effect of faculae on total irradiance while more than 90% of total irradiance is emitted from the photosphere. On one hand, the basic question is whether the area and position as well as the contrast of the chromospheric plages are the same as those of the photospheric faculae during the course of the evolution of active regions and over the solar cycle. On the other hand, as described by Fröhlich (2002), the ability of chromospheric proxies to track photospheric facular brightness changes on time scales of days to months is limited. It also should be noted that the Mg c/w ratio is a full-disk index and it is not yet known to what extent its variations (both short and longer term ones) are caused by plages and the network. Furthermore, it cannot be excluded that other effects that are not properly described by the current proxies also contribute to the residuals.

One of these effects may be related to some properties of active regions that are not taken into account in the model. To study the effect of various sunspot groups on TSI variations directly, we have to remove first the effect of faculae from the TSI values. For this purpose, we have calculated the $b*PSI$ values from equation of the model as follows: $b*PSI = TSI-(a+c*Mg_l+d*Mg_s) = TSI - (1325.113 + 147.35 * Mg_l + 104.006 * Mg_s)$.

The scatter plot between PSI and the TSI corrected for the effect of faculae is shown in Figure 2. It is reasonable to assume that various subsets of sunspot groups would result in different slopes of the regression line. To study the assumption we choose the TSI corrected for facular excess as our new dependent variable of the linear regression, and PSI is the independent variable in the selected cases. The variation of the b regression coefficient in the various cases may reveal some unknown effects related to sunspot groups.

3.2. Differences between sunspot classes due to the Zürich classification

An unsettled question is whether the evolution and/or morphology of active regions affect the depth and the shape of the sunspot-related dips in TSI. As shown by Pap (1985; 2003) and Fröhlich and Pap (1989) the evolving and complex groups are the main causes of the large temporary irradiance dips. Zahid et al. (2004) further investigated this question, however, their results were inconclusive since the small delta spot in their study was formed in the center of the disk and then the evolutionary and geometrical effects competed with each other as the spot moved toward the limb. In the following sections, we will show the results of our statistical study of whether and to what extent morphology and/or evolution of sunspot groups affects the depth of the dips.

Figure 1: Data used for the 1993-1998 time-interval: a) PSI, b) Measured Mg c/w, c) Long-term variation of Mg c/w, d) Short-term variation of Mg c/w, e) Measured total solar irradiance, f) Residuals of the multiple regression model.

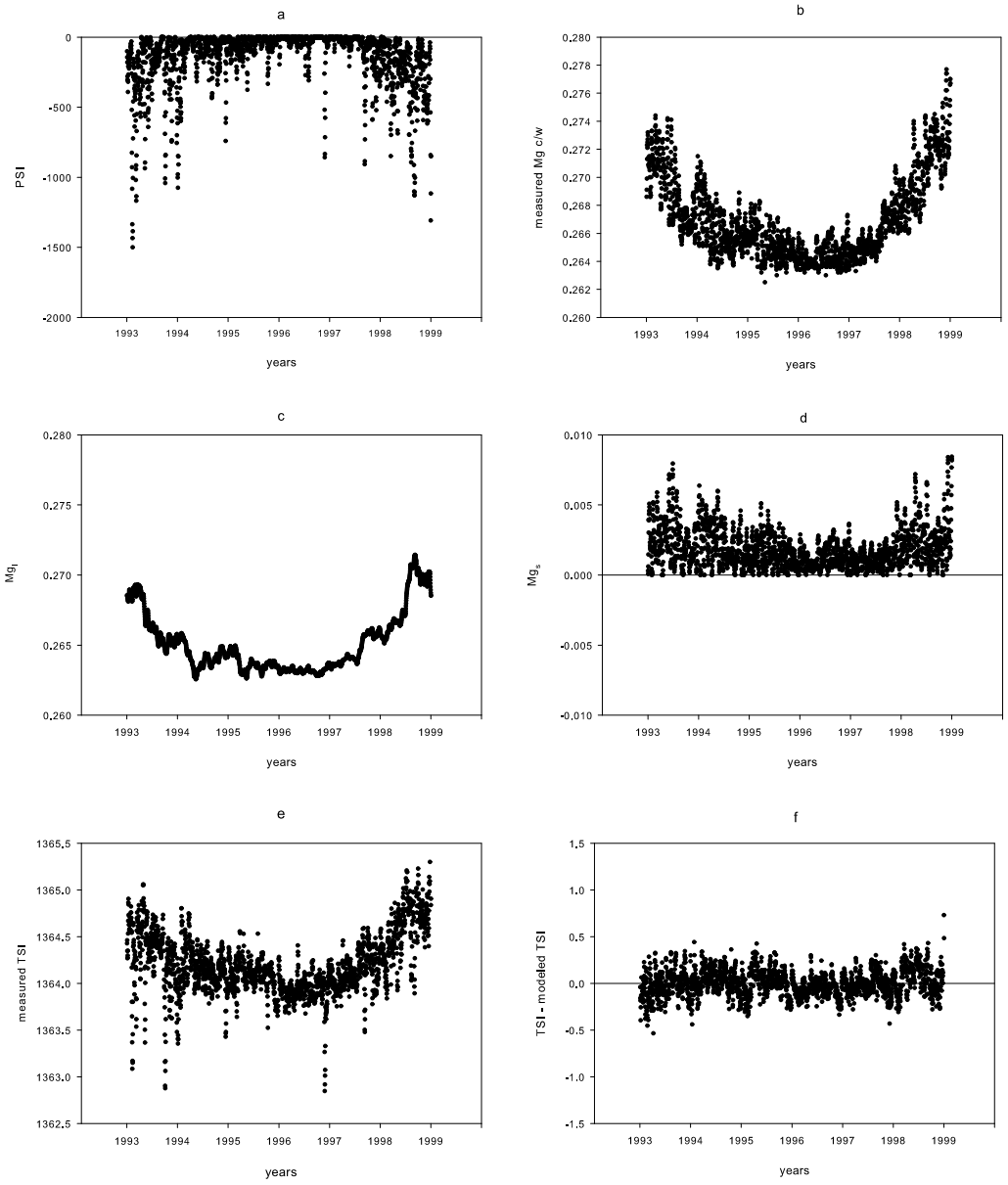

Figure 2: The TSI corrected for facular excess vs. PSI

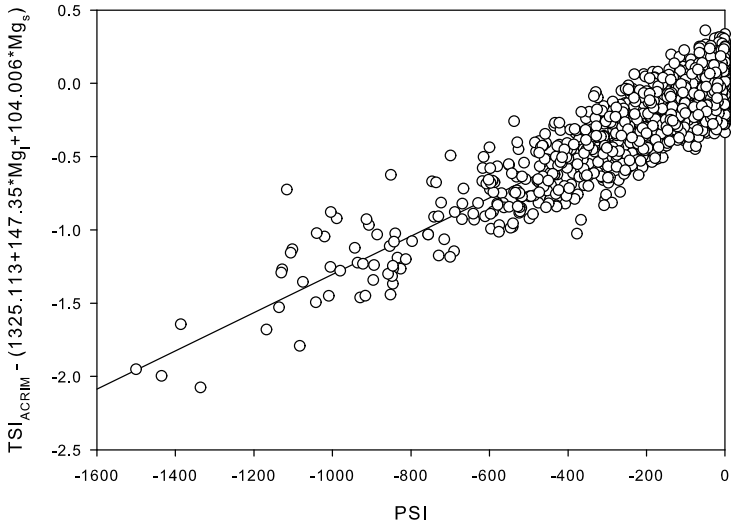

We first studied the dependence of the PSI values and their corresponding b values on the CMD of sunspot groups. We have divided the sunspot groups into three subsets according to their CMD of bins between 0 to 20, 20 to 40, and 40 to 60 degrees. The relation between the b values and the various Zürich classes depending on the CMD is shown in Figure 3. The error bars are the standard errors of the coefficients here and in all the following figures. As can be seen, the values of b depend on the type of the Zürich class. In the cases of $0 <= |CMD| < 20$ and $20 <= |CMD| < 40$ there is a decreasing trend of b, while in the case of $40 <= |CMD| < 60$ this trend cannot be seen (although the decreasing trend of b at class H seems to continue here). This trend may indicate to some effect of morphology of active regions and/or some evolutionary effect since the order of Zürich classes roughly follows the evolution of a large sunspot group.

3.3. Effect of magnetic configuration of sunspot groups

It cannot be excluded that the magnetic configuration of sunspot group also plays a role in the amplitude of the sunspot-related irradiance dips. To eliminate the effects of differences between the Zürich classes, the possible dependence of b on the magnetic configuration is studied by confining the dataset to sunspot groups of class E. There are three magnetic classes based

Figure 3: The b values calculated for PSI to model the TSI corrected for facular excess as a function of Zürich class and their Central Meridian Distance.

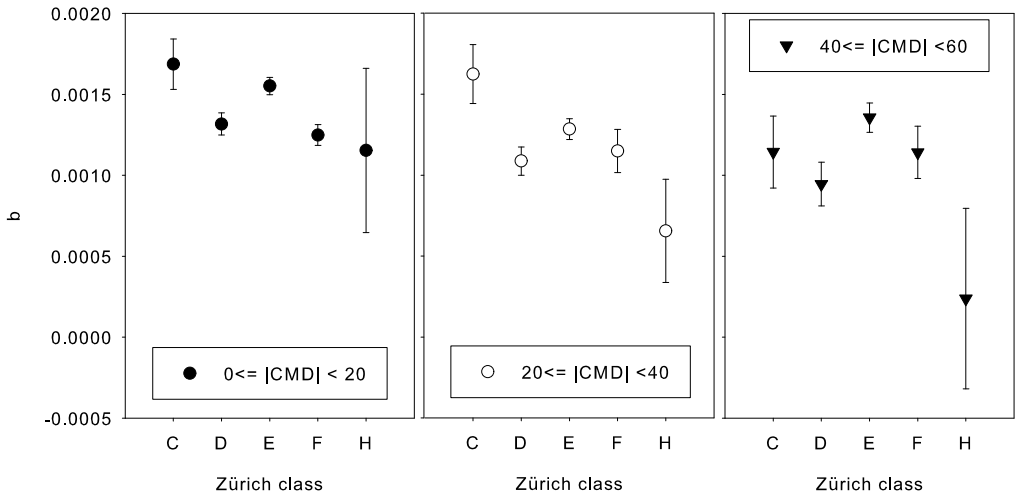

on the Mount Wilson magnetic classification scheme which are the most frequently used in SGD for the groups of class E showing their increasing magnetic complexity:

β: A sunspot group having both positive and negative magnetic polarities (bipolar), with a simple and distinct division between the polarities.

$\beta\gamma$: A sunspot group that is bipolar but which is sufficiently complex that no single, continuous line can be drawn between spots of opposite polarities.

$\beta\gamma\delta$: A sunspot group of beta-gamma magnetic classification but containing one or more delta spot(s) of umbrae separated by less than 2 degrees within one penumbra with opposite polarity.

We usually separated subsets of class E into the magnetic classes β, $\beta\gamma$ and $\beta\gamma\delta$ on the basis of SGD but in the ambiguous cases, especially in the case of class $\beta\gamma\delta$, the magnetic class was double-checked using the photospheric images and magnetograms appended to DPD, and it was corrected when it was necessary. The subsets of β, $\beta\gamma$ and $\beta\gamma\delta$ contain 37, 31, and 36 sunspot groups respectively within the central part of the solar disk ($0 <= |CMD| < 40$). The results of the appropriate b values against the magnetic configuration depending on the CMD are plotted in Figure 4, which shows a slight decrease of b with the increase of complexity.

Figure 4: The b multiplying factor for the subset of β, $\beta\gamma$ and $\beta\gamma\delta$ magnetic configuration of sunspot groups of Zürich class E in central part of the solar disk ($0 <= |CMD| < 40$).

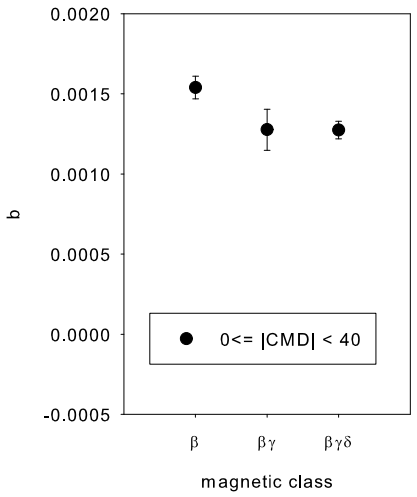

4. Discussion

The goal of the research described in this paper is to study the short-term variations in total solar irradiance at the time of relatively low level of solar activity, which allowed us to study how morphology and/or evolution of individual sunspot groups affect total irradiance. To directly compare the sunspot effect on total irradiance, we studied the variation of the b regression coefficient between the TSI corrected for facular brightening and PSI in the cases of various classes of sunspot groups. The selection criteria were the location, morphology (Zürich classes), and magnetic configuration of sunspot groups. The detailed study of the values of b shows a decreasing trend in the bin of $0 <= |CMD| < 40$: the value of b is the largest when the group is in class C, and it is the smallest for the old groups of class H. Since the consecutive Zürich classes roughly follow the stage of evolution of a large sunspot group, these results may indicate that the sunspot-related irradiance dips are influenced by the evolutionary stage of sunspot groups. Our results also indicate that the value of b slightly decreases with the increase of complexity of magnetic configuration of sunspot groups within a Zürich class.

To explain the found results various possible causes or contributors can be identified, such as (1) PSI-related effects, (2) facular effects, and (3) other

solar effects not taken into account in the model.

1. PSI-related effects: The sunspot evolution may contribute to changes in umbral intensity (Norton and Gilman, 2004). Therefore, a reasonable explanation for our findings would be that the contrast-area relationship changes during the evolution of sunspot groups.

2. Facular effects: Some of our results may be related to the fact that the disk-integrated chromospheric Mg c/w ratio is not able to model the photospheric facular effect properly, as already mentioned above, and the facular effects partially remain in the TSI corrected for facular excess. Ortiz et al. (2004) studied the facular contribution to solar irradiance variations of an isolated active region during several Carrington rotations, and they found that the total facular emission shows a decrease depending on aging probably due to the enlargement and spread out of the active region. On the basis of this result one can assume that a facular-related effect causes large changes with aging of the active regions and center-to-limb variation.

3. Other solar effects:

   (a) The found dependence on the aging of sunspot groups and variations of irradiance can also be explained by a delayed re-radiation mechanism of the missing energy in the sunspot-related irradiance dips. The decrease of b with aging may indicate that the surrounding quiet Sun may be brighter around these old simple groups than around the young developing groups, as suggested by Pap (1985; 1986) and Fröhlich and Pap (1989).

   (b) The decrease of b for $\beta\gamma$ and $\beta\gamma\delta$ groups in comparison with β groups may be related to the contributions of flares to TSI (Woods et al., 2004; Kretzschmar et al., 2010), because the more complex a group is the more often it is related to flares. The numerous small flares may contribute to the increase of TSI, and PSI has to account for smaller dips in these cases.

   (c) Some other types of effects (e. g. the contribution to the TSI from other spectral ranges) that are not properly described by the Mg c/w ratio and the PSI may also play some role.

The results are based on a relatively small statistical sample size, thus, they are not conclusive, and the underlying mechanisms cannot be revealed.

However, these results indicate that the raised questions might be worth a further careful analysis. The investigation should be extended to a larger period with an increased statistical sample size, and using spatially resolved facular data. To achieve this goal publications of detailed high time-resolution sunspot and photospheric facular catalogues are already started at the Heliophysical Observatory by using the SOHO/MDI and SDO/HMI data. Forthcoming high-resolution sunspot and facular data will provide new tools to draw reliable conclusions in the questions presented here.

5. Acknowledgements

This work was supported by the ESA PECS project No. C98081 (T.B.) and by NASA grant NNX09AB83G, supported by the Living With a Star Program (J.P.).

References

de Toma, G., White, O. R., Chapman, G. A., Walton, S. R., Preminger, D. G., Cookson, A. M., Harvey, K. L., Astrophys. J., 549, L131-L134, 2001

Domingo, V., Ermolli, I., Fox, P., Fröhlich, C., Haberreiter, M., Krivova, N., Kopp, G., Schmutz, W., Solanki, S. K., Spruit, H. C.; Unruh, Y., Vögler, A., Solar surface magnetism and irradiance on time scales from days to the 11-year cycle, Space Sci. Rev., 145, 337-380, 2009

Floyd, L., Newmark, J., Cook, J., Herring, L., McMullin, D., Solar EUV and UV spectral irradiances and solar indices, J. Atmos. Sol. Terr. Phys., 67, 3-15, 2005

Fröhlich, C., Total solar irradiance variations since 1978, Adv. Space Res., 29, 1409-1416, 2002

Fröhlich, C., Pap, J., Multispectral analysis of total solar irradiance variations, Astron. Astrophys., 220-272, 1989

Fröhlich C., Crommelynck D. A., Wehrli Ch., Anklin, M., Dewitte, S., Fichot, A., Finsterle, W., Jiménez, A., Chevalier, A., Roth, H., In-flight performance of the VIRGO solar irradiance instruments on SOHO, Solar Phys., 175, 267-286, 1997

Győri, L., Automation of area measurement of sunspots, Solar Phys., 180, 109-130, 1998

Győri, L., Baranyi, T., Ludmány, A., Photospheric data programs at the Debrecen Observatory, Proc. IAU Symp., 273, 403-407, 2011

Győri, L., Baranyi, T., Muraközy, J., Ludmány, A., Recent advances in the Debrecen sunspot catalogues, Mem. Soc. Astron. Ital., 76, 981-984, 2005

Heath, D.F., Schlesinger, B.M., The Mg 280-nm doublet as a monitor of changes in solar ultraviolet irradiance, J. Geophys. Res., 91, 8672-8682, 1986

Hudson, H.S., Silva, S., Woodard, M., Willson, R.C., The effects of sunspots on solar irradiance, Solar Phys., 76, 211-219, 1982

Kretzschmar, M., Dudok de Wit, T., Schmutz, W., Mekaoui, S., Hochedez, J., Dewitte, S., The effect of ares on total solar irradiance, Nature Physics, 6, 690-692, 2010

Krivova, N.A., Solanki, S.K., Unruh, Y.C., Towards a long-term record of solar total and spectral irradiance, J. Atmos. Sol.-Terr. Phys., 73, 223-234, 2011a

Norton, A.A., Gilman, P.A., Magnetic field-minimum intensity correlation in sunspots: A tool for solar dynamo diagnostics, Astrophys. J., 603, 348-354, 2004

Ortiz,A., Domingo, V., Sanahuja, B., Fröhlich, C., Excess facular emission from an isolated active region during solar minimum: the example of NOAA AR 7978, J. Atmos. Sol.-Terr. Phys., 66, 67-75, 2004

Pap, J., Activity of sunspots and solar constant variations during 1980, Solar Phys., 97, 21-33, 1985

Pap, J., Connection of the solar constant variations with the age and activity of sunspots, Adv. Space Res., 6, 65-68, 1986

Pap, J.: Variations in solar total and spectral irradiance and climate impact of solar variability, In The Sun's Surface and Subsurface (ed. J.P. Rozelot), Lecture Notes in Physics, Springer, 129-155, 2003

Pap, J. M., Turmon, M., Floyd, L., Fröhlich, C., Wehrli, Ch., Total solar and spectral irradiance variations from solar cycles 21 to 23, Adv. Space Res., 29, 1923-1932, 2002

Preminger, D.G., Walton, S.R., From sunspot srea to solar variability: A linear transformation, Solar Phys., 240, 17-23, 2007

Schmidt, G. A., Jungclaus, J. H., Ammann, C. M., Bard, E., Braconnot, P., Crowley, T. J., Delaygue, G., Joos, F., Krivova, N. A., Muscheler, R., Otto-Bliesner, B. L., Pongratz, J., Shindell, D. T., Solanki, S. K., Steinhilber, F., Vieira, L. E. A., Climate forcing reconstructions for use in PMIP simulations of the last millennium (v1.0), Geosci. Model Dev., 4, 33-45, 2011

Steinegger, M., Brandt, P. N., Schmidt, W., Pap, J., Sunspot photometry and the total solar irradiance deficit measured in 1980 by ACRIM, Astrophys. Space Sci., 170, 127-133, 1990

Vigouroux, A., Pap, J. M., Delache, P., Estimating long-term solar irradiance variability: A new approach, Solar Phys., 176, 1-21, 1997

Wesolowski, M.J., Walton, S.R., Chapman, G.A., The behavior of sunspot contrast during cycle 23, Solar Phys., 248, 141-154, 2008

Willson, R.C., Mordvinov, A.V., Secular total solar irradiance trend during solar cycles 21-23, Geophys. Res. Lett., 30 (5), 1199, doi:10.1029/2002GL016038, 2003

Zahid, H. J., Hudson, H. S., Fröhlich, C., Total solar irradiance variation during rapid sunspot growth, Solar Phys., 222, 1-15, 2004